ISBN: 978-3-95450-247-9 ISSN: 2673-5490 doi: 10.18429/JACoW-IPAC2024-MOPR38

AN LWFA INJECTOR FOR AWAKE RUN 2 EXPERIMENT

Samuel Marini*[1], Damien F. G. Minenna[1], Francesco Massimo[2], Laury Batista[1], Vittorio Bencini[3], Antoine Chancé[1], Nicolas Chauvin[1], Steffen Doebert[3], John Farmer[4], Edda Gschwendtner[3], Ioaquin Moulanier[2], Patric Muggli[4], Didier Uriot[1], Brigitte Cros[2], Phu Anh Phi Nghiem[1]
[1]CEA, IRFU, DACM, Université Paris-Saclay, 91191 Gif-sur-Yvette, France
[2]LPGP, CNRS, Université Paris-Saclay, 91405 Orsay, France
[3]CERN, Geneva, Switzerland
[4]Max Planck Institute for Physics, Munich, Germany

Abstract

A beam physics design has been carried out for a 200 MeV-LWFA injector to the AWAKE Run 2 experiment as an alternative to the baseline radio frequency (RF) injectors. It is composed of a laser-plasma acceleration section and a transport line. In addition to specific environment constraints that impose a dogleg configuration, the electron beam must feature unprecedented performances for a plasma-based accelerator: 100 pC charge, a few μm rad emittance, and a few % energy spread. Thanks to an integrated beam physics study, assigning specific roles to each section of the accelerator, all the requirements are successfully met, paving the way for plasma-based accelerators to be competitive with conventional accelerators.

INTRODUCTION

Laser Wakefield Acceleration (LWFA) is a promising technique for developing compact electron sources. However, transitioning LWFA from experimental setups to functional accelerators with dedicated applications requires the electron beam quality to meet specific characteristics, not at the plasma exit but at the application itself.

The injector of the EARLI (Electron Accelerator driven by a Reliable Laser Wakefield for Industrial uses) project must provide a 200 MeV electron beam to the AWAKE Run 2 experiment with very challenging requirements on beam charge, size and emittance as listed in Table 1. In addition, environment constraints impose the use of a dogleg transport line to drive the beam to the injection point (see Fig. 1). The EARLI project aligns with initiatives such as EuPRAXIA [1], aiming to develop compact electron sources with broad applications, ranging from light and particle sources to medical research.

To meet these unprecedented performances for a plasma based accelerator, we apply beam physics studies analogous to those for a conventional accelerator [2], where laser-plasma acceleration and transport sections are studied in an integrated way, by assigning precise roles to each of them. The role of the laser-plasma acceleration section is to produce and deliver a beam at a given energy, charge and emittance with enough margin, knowing that these features deteriorated in the downstream transport line. In addition, according to [3], for limiting emittance growth in the transport line, the energy spread must be limited to a few percent, and the Twiss parameter $\gamma_{x,y}$, limited to a few hundreds of m^{-1} at the plasma exit. The role of the transport line is then to capture the beam exiting from the plasma cell properly and subsequently fine tune it to obtain the sizes and divergences, all while minimizing emittance deterioration to fulfill all the requirements.

In the next sections, we present the laser-plasma and then the transport line configurations obtained from beam physics and massive numerical simulations, following the objectives assigned above.

Table 1: Top-level Requirements on Beam Parameters at the EARLI Injector Exit

Beam parameter	Top-level requirements
Charge Q	$\geqslant$ 100 pC
Mean energy E	100 – 250 MeV
Norm. emittance $\epsilon_{x,y}$	$\leqslant$ 2 μm rad
Beam size $\sigma_{x,y}$	6 μm
Twiss, $\alpha_{x,y}$, $D_{x,y}$, and $D'_{x,y}$	0

LASER-PLASMA ACCELERATION SECTION

The laser pulse is linearly polarized in the x-direction and features a flattened Gaussian transverse intensity profile, with $N = 6$ as the flatness parameter [4]. The laser focal

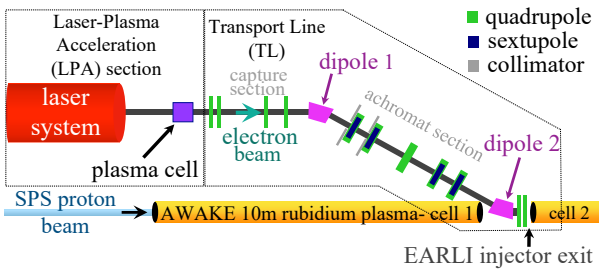

Figure 1: Schematic layout of the EARLI laser-plasma based electron injector to be inserted into the AWAKE environment. The electrons generated in the laser-plasma acceleration section (box on the left) are transported in the transport line (box on the right) up to the gap between the two rubidium plasma cells.

* samuel.marini@cea.fr

ISBN: 978-3-95450-247-9 ISSN: 2673-5490 doi: 10.18429/JACoW-IPAC2024-MOPR38

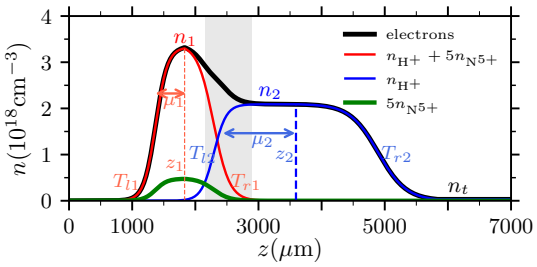

Figure 2: Longitudinal plasma density profile in a three-zone plasma cell. The first zone contains a hydrogen-nitrogen plasma mixture, with hydrogen shown in red and nitrogen (enhanced 5x for visibility) in green. The second and third zones contain hydrogen plasma, represented by the blue curve. The density in the third zone is ∼ 100 times lower than in the second. The black curve depicts the total plasma density, while the gray region highlights areas of nitrogen ionization.

position z_f, the peak field amplitude a_0, waist w_0 and the field duration τ_0 are selected to maintain a weakly nonlinear laser-plasma interaction while still generating a wakefield strong enough to accelerate a substantial amount of charge to the required final energy.

The plasma's longitudinal density profile is structured into two main plateaus, n_1 and n_2, and a lower density tail n_t, forming a three-zone plasma cell described by $f(z) = n_1 s_1(z) + n_2 s_2(z) + \Theta(z - z_2)\Theta(n_t - n_2 s_2(z))\,(n_t - n_2 s_2(z))$, where Θ is the Heaviside step function, and the functions s_α, with $\alpha = 1$ or 2 are given by a double-normalized Fermi-Dirac function $s_\alpha(z) = \dfrac{1+\exp(-\mu_\alpha/T_{l\alpha})}{1+\exp(-(\mu_\alpha+z-z_\alpha)/T_{l\alpha})}$, if $z < z_\alpha$ and $s_\alpha(z) = \dfrac{1+\exp(-\mu_\alpha/T_{r\alpha})}{1+\exp(-(\mu_\alpha-z+z_\alpha)/T_{r\alpha})}$, if $z \geq z_\alpha$ where z_α is the central position of the plateau, μ_α its length, and $T_{l\alpha}$ (respectively, $T_{r\alpha}$) represents the density variation rate on the left (respectively, right) plateau side.

The plasma configuration is thus defined by twelve parameters that require optimization, with key parameters such as the density and length of the main plateau, *i.e.*, n_2 and μ_2, first estimated using scaling laws [5]. Assuming the initial laser's parameters $a_0 \sim 1.5$, $w_0 \sim 20$ μm, $\tau_0 \sim 25$ fs, and the blowout regime, n_2 ranges from 3×10^{23} m^{-3} to 3×10^{24} m^{-3}, and the corresponding dephasing length, μ_2, spans from 2500 μm to 3500 μm. With these ideal conditions and beam loading, Refs. [5,6] suggest that hundreds of pC charge can be accelerated to energies of hundreds MeV, aligning with the EARLI injector's requirements.

Initially, the laser pulse front ($I < 10^{18}$ Wcm^{-2}) partially ionizes the gas, creating a plasma (see Fig. 2) with electron contributions from hydrogen (one per atom) and nitrogen (five per atom from the external L atomic shell). As the laser pulse enters the plasma, it is self-focused and compressed, changing its peak field intensity according to the plasma density profile. The plasma is classified into three distinct zones.

In the first plasma zone ($z \lesssim 3000$ μm), nitrogen is present, and the laser pulse can get strong $a_0 > 1.5$, ionizing electrons from the inner shells of nitrogen, which are eventually captured in the wakefield bubble, giving rise to the electron beam. There, the beam emittance is set. It is higher in the laser pulse's polarization plane due to oscillations of the electric field vector **E**. Low emittance requires a small field amplitude, whereas, in opposition, high charge necessitates a larger field amplitude.

In the second plasma zone (3000 μm$\lesssim z \lesssim$ 4500 μm), only hydrogen is present. There, electrons trapped in the wakefield bubble are significantly focused and accelerated to hundreds of MeV. The electric field is determined by the bubble which is generated by ponderomotive forces that depend on the field gradient amplitude squared $|\nabla\mathbf{E}|^2$. Since the latter present cylindrical symmetry, the ratio ϵ_x/ϵ_y stays nearly constant, and the Twiss parameters $(\alpha, \beta, \gamma)_{x,y}$ are nearly identical in both x and $y-$directions. Strong focusing forces significantly reduce beam's transverse size while $\gamma_{x,y}$ reads $\sim 10^3$ m^{-1}. Energy spread usually reduces during acceleration but can increase due to longitudinal wakefield variations along the bunch length. Since high charge results in longer bunch length, there is a competition between high charge and low energy spread.

The third plasma zone ($z \gtrsim 4500$ μm) is characterized by low-density hydrogen where focusing forces are moderate and acceleration is negligible. The bunch's transverse size increases while $\gamma_{x,y}$ values decrease to $\sim 10^2$m^{-1}.

Table 2: Laser and Plasma Parameters used to Obtain the Candidate Solution from the LPA Simulation

Laser parameters		Plasma parameters	
a_0	1.36	z_1, z_2	1830, 3594 μm
w_0	20.9 μm	μ_1, μ_2	458, 1300 μm
τ_0 (field)	25 fs	T_{r1}, T_{l1}	93, 127 μm
z_f	3700 μm	T_{r2}, T_{l2}	99, 223 μm
		n_1	3.30×10^{24} m^{-3}
		n_2	2.09×10^{24} m^{-3}
		$n_{N^{5+}}$	0.953×10^{23} m^{-3}
		n_t	0.300×10^{23} m^{-3}

Each of these three plasma zones influences distinct transverse and longitudinal beam characteristics, requiring massive simulations and optimizations, which are conducted using the FBPIC particle-in-cell [4]. Among several interesting solutions, we identify the laser-plasma configuration outlined in Table 2 as the most encouraging. The characteristics of the resulting electron beam include a charge of 128 pC, mean energy of 194 MeV, energy spread (RMS) of 3.6%, normalized emittances ϵ_x and ϵ_y of 3.2 and 0.6 μm rad respectively, Twiss parameters $\gamma_{x,y}$ around 467 m^{-1}, and beam sizes (1-RMS) σ_x and σ_y of 4.71 and 1.89 μm respectively. Ref. [2] suggests that slight variations in individual laser-plasma parameters, on the order of a few percent, do not significantly alter beam properties and can be compensated by adjustments in other parameters.

ISBN: 978-3-95450-247-9 ISSN: 2673-5490 doi: 10.18429/JACoW-IPAC2024-MOPR38

TRANSPORT LINE SECTION

Efforts are focused on damping the very strong nonlinearities induced by the beam emittance and energy spread that are several orders of magnitude higher than in conventional accelerators. These issues are made worse when a strong focusing gradient must be applied to obtain smaller, micrometric beam sizes at the transport line exit.

The figure of merit considered is the beam emittance.

Following the guidelines for the EuPRAXIA project [1, 3], we placed two strong (~ 300 T/m), short (50 mm) quadrupoles made of permanent magnets near the plasma cell to reduce the Twiss $\gamma_{x,y}$ and control emittance growth (see Fig. 3). Another pair of strong and short quadrupoles at capture section reduces the beam size to $\sigma_{x,y} \sim 100\ \mu$m at the achromat entrance.

In the achromat section, to narrow as far as possible the growth of the dispersion function and, therefore, the emittance growth, short dipoles with reasonable field (150 mm, ~ 1 T) are used, with five quadrupoles strategically placed so that they require minimal strengths (150 mm, ~ 10 T/m).

Moreover, sextupoles are needed to correct nonlinear focusing defects that induce emittance growth. The most effective is to place sextupoles (i) within the quadrupoles or closest to them to correct the aberrations at their source, and (ii) where the dispersion function is the highest, *i.e.,* where particles of higher energies are farther from the central axis and thus can be more focused by sextupoles. Consequently, we used four sextupoles placed within the four quadrupoles in the achromat (the dispersion function is close to zero at the achromat central quadrupole). The resulting needed gradient is modest (~ 50 T/m^2).

An additional method to mitigate nonlinearities is to remove particles with highest off-energy using a collimator located at the first quadrupole of the achromat section, close to the region where both the dispersion function and the correlation between horizontal position and energy are maximum. A second collimator at the second quadrupole of the achromat section was used to remove particles far from the center in the transverse plane.

To achieve the required few micrometer beam size at the transport line exit, more two strong (~ 300 T/m) and short (50 mm) quadrupoles made of permanent magnets are added downstream of the achromat section.

Based on the above strategy dictated by beam physics considerations, massive simulations and optimizations with the TraceWin code [7] allowed to obtain beam parameters meeting all the requirements listed in Table 1, as specified in Table 3.

Table 3: Top-level Requirements on Beam Parameters at the EARLI Injector Exit

Beam parameter	EARLI injector exit
Charge Q	$\geqslant$ 100 pC
Mean energy E	194 MeV
Norm. emittance ϵ_x, ϵ_y	4, 0.7 μm.rad
Beam size σ_x, σ_y	4.8, 6.0 μm
Twiss, $\alpha_{x,y}$, $D_{x,y}$, and $D'_{x,y}$	~ 0

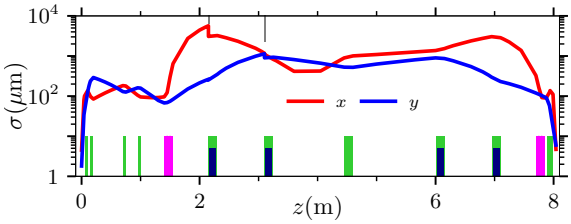

Figure 3: Transverse beam envelopes (1−RMS) along the transport line. Dipoles are in purple, quadrupoles in green, sextupoles in black, and collimators in gray.

CONCLUSION

We have shown how consistent strategies based on beam physics and massive numerical optimizations allow the design of an accelerator able to deliver electron beams with the quality required by the AWAKE run 2 experiment, while also offering potential for diverse applications requiring high quality and energetic electron bunches.

ACKNOWLEDGEMENTS

This work was performed using HPC resources from GENCI-IDRIS (Grant 2022-A0130510062) and from the Grant CCRT2023-minennda awarded by the Fundamental Research Division (DRF) of CEA. The authors are grateful to DACM/CEA team for fruitful discussions.

REFERENCES

[1] R. W. Assmann *et al.,* "EuPRAXIA Conceptual Design Report," *Eur. Phys. J. Spec. Top.*, vol. 229, pp. 3675-4284, Dec. 2020. doi:10.1140/epjst/e2020-000127-8

[2] S. Marini *et al.,* "Beam physics studies for a high charge and high beam quality laser-plasma accelerator," *Phys. Rev. Accel. Beams*, accepted, 2024.

[3] X. Li, A. Chancé, and P. A. P. Nghiem, "Preserving emittance by matching out and matching in plasma wakefield acceleration stage,"*Phys. Rev. Accel. Beams*, vol. 22, no. 2, Feb. 2019. doi:10.1103/physrevaccelbeams.22.021304

[4] R. Lehe *et al.,* "A spectral, quasi-cylindrical and dispersion-free Particle-In-Cell algorithm,"*Comput. Phys. Commun.*, vol. 203, pp. 66–82, Jun. 2016, https://fbpic.github.io , doi:10.1016/j.cpc.2016.02.007

[5] W. Lu *et al.,* "Generating multi-GeV electron bunches using single stage laser wakefield acceleration in a 3D nonlinear regime," *Phys. Rev. Accel. Beams,* vol. 10, no. 6, p. 061301, Jun. 2007. doi:10.1103/PhysRevSTAB.10.061301

[6] J. P. Couperus *et al.,* "Demonstration of a beam loaded nanocoulomb-class laser wakefield accelerator," *Nat. Commun.*, vol. 8, no. 1, p. 487, Sep. 2017. doi:10.1038/s41467-017-00592-7

[7] D. Uriot and N. Pichoff, "Status of TraceWin Code", in *Proc. IPAC'15*, Richmond, VA, USA, May 2015, pp. 92–94. doi:10.18429/JACoW-IPAC2015-MOPWA008